Genome-wide gene expression changes associated with exposure of rat liver, heart, and kidney cells to endosulfan

Ruifeng Liu[a,1], Richard L. Printz[b,1], Erin C. Jenkins[b], Tracy P. O'Brien[b], Jerez A. Te[a], Masakazu Shiota[b], Anders Wallqvist[a,*]

[a] Department of Defense Biotechnology High Performance Computing Software Applications Institute, Telemedicine and Advanced Technology Research Center, US Army Medical Research and Materiel Command, Fort Detrick, MD 21702, USA
[b] Department of Molecular Physiology and Biophysics, Vanderbilt University School of Medicine, Nashville, TN 37232, USA

ARTICLE INFO

ABSTRACT

Endosulfan was once the most commonly used pesticide in agriculture and horticulture. It is an environmentally persistent organochlorine compound with the potential to bioaccumulate as it progresses through the food chain. Its acute and chronic toxicity to mammals, including humans, is well known, but the molecular mechanisms of its toxicity are not fully understood. To gain insight to these mechanisms, we examined genome-wide gene expression changes of rat liver, heart, and kidney cells induced by endosulfan exposure. We found that among the cell types examined, kidney and liver cells were the most sensitive and most resilient, respectively, to endosulfan insult. We acquired RNA sequencing information from cells exposed to endosulfan to identify differentially expressed genes, which we further examined to determine the cellular pathways that were affected. In kidney cells, exposure to endosulfan was uniquely associated with altered expression levels of genes constituting the hypoxia-inducible factor-1 (HIF-1) signaling pathway. In heart and liver cells, exposure to endosulfan altered the expression levels of genes for many members of the extracellular matrix (ECM)-receptor interaction pathway. Because both HIF-1 signaling and ECM-receptor interaction pathways directly or indirectly control cell growth, differentiation, proliferation, and apoptosis, our findings suggest that dysregulation of these pathways is responsible for endosulfan-induced cell death.

1. Introduction

Once commonly used as a pesticide for agriculture and horticulture, endosulfan is now banned or scheduled to be phased out in more than eighty counties because it belongs to a class of environmentally hazardous compounds called organochlorines with the alpha-isomer of endosulfan being more toxic than the beta-isomer (Maier-Bode, 1968). These compounds are environmentally persistent, non-biodegradable, and possess biomagnification potential, because their organismal concentrations can accumulate as they move up through the food chain. Studies of endosulfan have shown deleterious effects on the health of aquatic organisms at concentrations above 0.22 or 0.056 μg/L with acute or chronic exposure, respectively (Mersie et al., 2003). Its biomagnification potential is extremely high; for example, even when present at low levels, this pesticide can effectively accumulate within a fish and cause numerous toxic effects that result in physiological, biochemical, and molecular alterations, tissue damage, and ultimately

death (Jonsson and Toledo, 1993). It is well known that occupational exposure to endosulfan can lead to malaise, nausea, vomiting, dizziness, confusion, and convulsions (Ely et al., 1967). Alarmingly, endosulfan has been found in human breast milk, which suggests the possibility that the toxin is transferred from mother to infant (Lutter et al., 1998). According to animal studies and case reports of human poisoning, acute oral exposure to lethal or near-lethal amounts of endosulfan damages many organs, including the brain, lung, kidney, and liver (Demeter and Heyndrickx, 1978). There are no chronic exposure studies in humans. However, in rats, long-term sub-lethal exposure appears to affect the kidney as the primary systemic target organ (Reuber, 1981).

Owing to environmental concerns and its adverse effects on human health, endosulfan has been the subject of numerous toxicology studies. Despite these efforts, the molecular mechanisms of endosulfan toxicity are still not fully elucidated. Several cellular and molecular mechanisms of endosulfan toxicity have been proposed. Based on studies of endosulfan-induced apoptosis in a human leukemic T-cell line, Kannan

(Kannan et al., 2000) and Jain (Kannan and Jain, 2003) proposed oxidative stress and mitochondrial dysfunction induced by endosulfan exposure as key molecular initiating events of endosulfan-induced T-cell apoptosis. The role of oxidative stress was confirmed by Sohn et al. in *Saccharomyces cerevisiae* as well as human HepG2 and HeLa cell lines, which showed that lipid-soluble antioxidants had a protective effect against endosulfan-induced oxidative damage (Sohn et al., 2004). Song et al. also investigated endosulfan toxicity in HepG2 cells and proposed that endosulfan increases oxidative stress-responsive transcription via activating protein-1 (Song et al., 2012).

The effects of endosulfan exposure have also been investigated in other cell types. Kim et al. studied the influence of endosulfan on cyclooxygenase-2 (COX-2) expression in murine macrophage RAW264.7 cells and concluded that it induces COX-2 expression via the NADPH oxidase, reactive oxygen species (ROS), and Akt/mitogen-activated protein kinase (MAPK) pathways (Kim et al., 2015). Li et al. exposed human umbilical vein endothelial cells to endosulfan and found increased secretion and mRNA expression levels of the inflammation factors interleukin (IL)-6 and IL-8 (Li et al., 2015). More recently, Zhou and coworkers investigated the effects of endosulfan exposure on multiple vital cellular processes in a variety of different cells. They found that in rat spermatogenic cells, endosulfan inhibits meiosis by reducing the expression of key regulatory factors leading to cell cycle arrest (Guo et al., 2016); in human umbilical vein endothelial cells, it inhibits proliferation through the Notch signaling pathway (Wei et al., 2017); and in human umbilical vascular cells, it induces apoptosis and necroptosis through activation of receptor-interacting protein kinase (RIPK) signaling (Zhang et al., 2017b), as well as autophagy and endothelial dysfunction via the 5′ adenosine monophosphate-activated protein kinase (AMPK)/mechanistic target of rapamycin (mTOR) signaling pathways (Zhang et al., 2017a).

Most studies published to date have limited their investigations of the impact of endosulfan exposure to a few specific genes or molecular pathways. To greatly expand the number of genes and pathways to test for possible effects arising from endosulfan exposure, we measured genome-wide changes of gene expression in rat hepatocytes, cardiomyocytes, and renal cells, using state-of-the-art RNA sequencing (RNA-seq) technology, with the aim of predicting the key cellular pathway perturbations induced by endosulfan exposure.

2. Materials & methods

2.1. Cell culture

Commercially available cryopreserved rat primary cells were used. Rat hepatocytes were obtained from Triangle Research Labs (RSD211; Research Triangle Park, NC). Hepatocytes were cultured in 96-well (clear, 354407) or 6-well (clear, 354400) collagen coated plates (Corning Life Sciences, Corning, NY). Cryopreserved rat hepatocytes, cultured as described by the supplier (Triangle Research Labs), were thawed, washed in a 50-ml conical tube of thawing medium (MCRT50, Triangle Research Labs), and plated into 96-well plates for endosulfan dose optimization or 6-well plates for RNA isolation, using plating medium (MP100, Triangle Research Labs). These plates of hepatocytes were incubated at 37 °C in a 5% CO$_2$ incubator for 5 h to allow cell attachment before the medium was replaced with maintenance medium (MM250, Triangle Research Labs). The next day, the hepatocytes were treated for the indicated times and doses with alpha-endosulfan (45468, Sigma-Aldrich, St. Louis, MO), prepared in DMSO prior to dilution in maintenance medium (final DMSO concentration was 0.5% for all treatments) (Table 1).

Rat renal proximal tubular epithelial cells (R4100) and rat cardiac myocytes (R6200) were obtained from ScienCell Research Laboratories (Carlsbad, CA). Rat renal cells and cardiomyocytes were cultured in 96-well (clear, 354461) or 6-well (clear, 354413) poly-D-lysine coated plates (Corning Life Sciences). Cryopreserved rat renal cells and

Table 1
Concentrations of endosulfan applied to different cells for 24 h to acquire RNA-seq data. These concentrations were selected as indicated by the results of lactate dehydrogenase leakage and cellular NADH/NADPH viability assays.

Cell type	Low dose (μM)	High dose (μM)
Cardiomyocytes	10	20
Hepatocytes	40	60
Renal proximal tubular epithelial cells	5	10

cardiomyocytes were placed into culture as described by the supplier (ScienCell Research Laboratories). Briefly, cells were thawed and plated into 96-well plates for endosulfan dose optimization or 6-well plates for RNA isolation, using epithelial cell medium (4131, ScienCell Research Laboratories) for renal cells or cardiac myocyte medium (6101-prf, ScienCell Research Laboratories) for cardiomyocytes. These plates of renal cells and cardiomyocytes were incubated at 37 °C in a 5% CO$_2$ incubator for 5 h to allow cell attachment before the medium was replaced. The next day, the renal cells or cardiomyocytes were treated with endosulfan (prepared as described above but diluted in the appropriate cell-type specific medium) for the indicated times and doses (Table 1).

2.2. Cell viability assays

The cytotoxicity of endosulfan on rat hepatocytes, cardiomyocytes, and renal cells was evaluated by two methods. The Cell Counting Kit-8 assay (Dojindo Molecular Technologies, Rockville, MD) was used for cells cultured in 96-well plates, as described by the manufacturer, to quantify cellular NADH/NADPH levels, which depend on the number of viable cells. A tetrazolium salt, WST-8, was reduced to form a colored WST-8 formazan dye and the absorbance at 450 nM was measured. The percent viability was calculated by taking the ratio of the absorbance for endosulfan-treated cells to that for an initially equivalent number of vehicle-treated cells. The Lactate Dehydrogenase (LDH) Activity Assay Kit (Sigma-Aldrich) was used to measure the amount of LDH released from cells into the culture medium after endosulfan exposure. As described by the manufacturer (Sigma-Aldrich), equivalent amounts of cell culture medium from endosulfan-treated and untreated cells cultured in 96-well clear plates were assayed, and the amount of LDH released was expressed as the ratio of the amount released by endosulfan-treated cells to that released by control (untreated) cells.

2.3. RNA isolation and sequencing

Total RNA was isolated from cultured primary cells, hepatocytes, cardiomyocytes, or renal cells, using TRIzol Reagent (Thermo Fisher Scientific, Waltham, MA) and the Direct-zol RNA MiniPrep kit (Zymo Research, Irvine, CA). The isolated RNA samples were then submitted to the Vanderbilt University Medical Center VANTAGE Core (Nashville, TN) for RNA quality determination and sequencing. Total RNA quality was assessed using a 2100 Bioanalyzer (Agilent, Santa Clara, CA). At least 200 ng of DNase-treated total RNA with high RNA integrity was used to generate poly-A-enriched mRNA libraries, using KAPA Stranded mRNA sample kits with indexed adaptors (Roche, Indianapolis, IN). Library quality was assessed using the 2100 Bioanalyzer (Agilent), and libraries were quantitated using KAPA Library Quantification Kits (Roche). Pooled libraries were subjected to 75-bp single-end sequencing according to the manufacturer's protocol (Illumina HiSeq3000, San Diego, CA). Bcl2fastq2 Conversion Software (Illumina) was used to generate de-multiplexed Fastq files.

2.4. Analysis of RNA-seq data

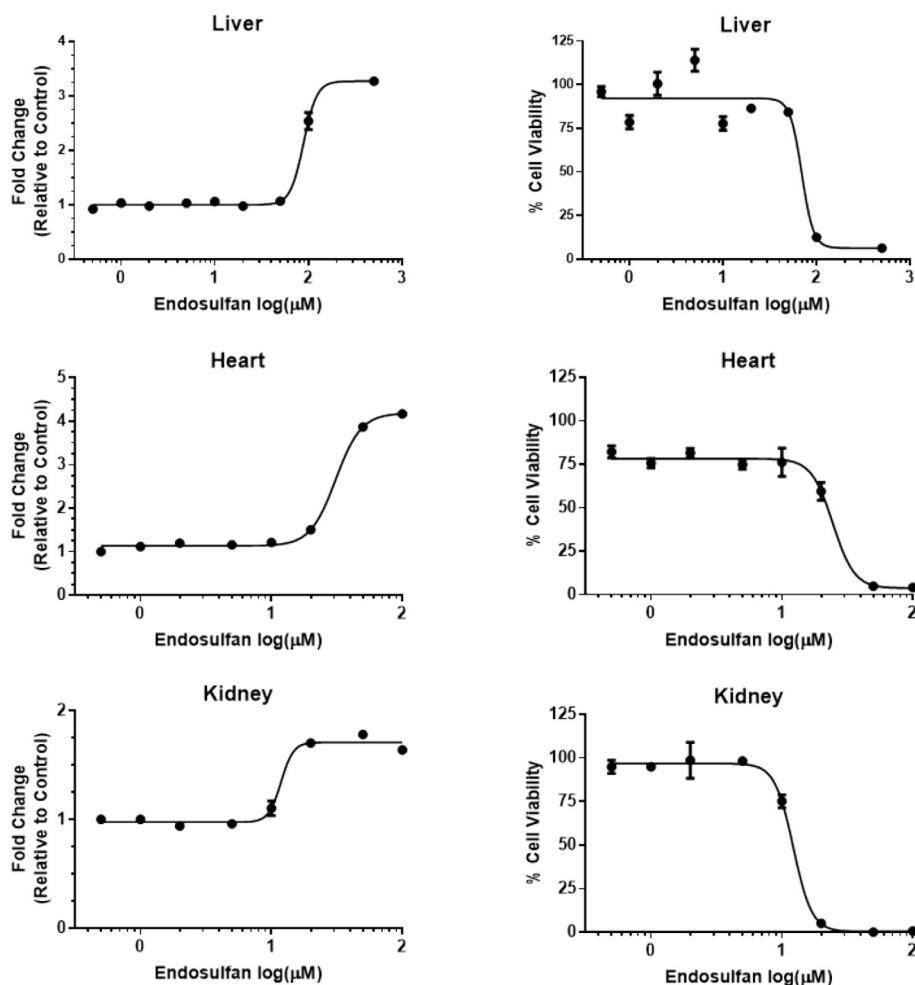We analyzed RNA-seq data with Kallisto, a recently developed RNA-

Fig. 1. Results of lactate dehydrogenase leakage (left column) and cellular NADH/NADPH viability (right column) assays to examine the cytotoxic effects of different endosulfan doses on rat liver, heart, and kidney cells. Nonlinear regression analysis (variable slope, four parameters) using GraphPad Prism 7 software was performed to fit curves to each semi-log plot of the mean fold change of LDH release relative to control cells ± SE (n = 3; left column) or mean % cell viability relative to control cells ± SE (n = 3; right column) at each endosulfan concentration tested. The estimated EC_{50} values from the nonlinear regression analysis of LDH release assays for liver, heart and kidney cells were 89, 31 and 12 μM, respectively. The estimated IC_{50} values from the nonlinear regression analysis of cellular NADH/NADPH viability assays for liver, heart and kidney cells were 69, 25 and 12 μM, respectively.

seq data analysis tool for read alignment and quantification. Kallisto pseudo-aligns reads to a reference, producing a list of transcripts that are compatible with each read while avoiding alignment of individual bases (Bray et al., 2016). In this study, we pseudo-aligned the reads to the rat transcriptome downloaded from the Kallisto website (http://bio.math.berkeley.edu/kallisto/transcriptomes/). Kallisto achieves a level of accuracy similar to that of other methods but is orders of magnitude faster; this allows calculating the uncertainty of transcript abundance estimates via the bootstrap technique of repeating analyses after re-sampling with replacement from the data. In this study, we employed bootstrapping by repeating analyses 100 times with resampling for each data set. Considering that the average number of reads per data set is 35 million (25 to 51 million single-end reads), using other software tools to perform the same bootstrap analysis becomes prohibitively expensive.

To identify differentially expressed genes (DEGs) from transcript abundance data quantified by Kallisto, we used a companion tool called Sleuth, which uses the results of the bootstrap analysis during transcript quantitation to estimate the technical variance directly for each sample (Pimentel et al., 2016). Many software tools for differential gene expression analysis of RNA-seq experiments assume that the technical variance of gene counts follows a Poisson distribution, in which the variance equals the mean (Oberg et al., 2012). However, for many genes, the technical variance can be much higher than the expected Poisson variance (McIntyre et al., 2011). A distinct advantage of Sleuth is that it models biological and technical variances explicitly with a response error model.

To understand the biological significance of the lists of genes whose expression levels were altered by endosulfan exposure (see Table S1 of the Supplemental Materials), we mapped the DEGs derived from

Kallisto-Sleuth analyses onto KEGG pathways to identify molecular pathways significantly enriched by endosulfan exposure. We used the online tool Database for Annotation, Visualization, and Integrated Discovery (DAVID) (Huang et al., 2009) to perform this task.

2.5. Quantitative PCR

Real-time quantitative PCR (qPCR) analysis was performed on several DEGs that were identified by RNA-seq to confirm the observed endosulfan induced changes in gene expression. For qPCR analysis, representative DEGs of known metabolic relevance were selected from various aspects of our studies, from key pathways in kidney, heart and liver cells identified by KEGG pathway enrichment analysis, from the group of DEGs common among all three cell types, or from the initial lists of DEGs identified by RNA-seq as having comparatively large differences in expression with endosulfan exposure. Total RNA samples that were isolated for the RNA-seq analysis from hepatocytes, cardiomyocytes or renal cells were also used to generate cDNA following the protocol for the High-Capacity cDNA Reverse Transcription Kit (Thermo Fisher Scientific). A CFX96 real-time PCR instrument and SsoAdvanced Universal SYBR Green Supermix (Bio-Rad, Hercules, CA) were used with approximately 10 (hepatocytes or cardiomyocytes) or 2 (renal cells) ng of cDNA and 0.1 μM of rat gene specific validated primer sets from RealTimePrimers.com (Elkins Park, PA) or custom designed then synthesized (Sigma-Aldrich) (see Table S2 of the Supplemental Materials for qPCR primer sequences). The real-time PCR program for gene amplification and expression detection consisted of 45 cycles of 95 °C for 10 s and 58 °C for 45 s. Real-time qPCR data were analyzed using the ΔΔCt method and the relative expression level of

each gene of interest was obtained by normalizing to the expression level of Rpl13a. Differential gene expression data is reported as ln(FC), where FC is the fold change in gene expression of endosulfan-treated cells relative to control (vehicle-treated) cells.

3. Results

3.1. Optimization of endosulfan doses

To estimate the optimal endosulfan doses for our studies on primary cultures of rat liver, heart and kidney cells, we examined the cytotoxic effects of increasing endosulfan concentration by measuring the release of lactate dehydrogenase (LDH) from damaged cells into the cell culture medium and the effects on cell viability by measuring NADH/NADPH levels present in metabolically active cells. The results are presented in Fig. 1 with the semi-log plots in the left column illustrating the fold changes in the amount of LDH released from cells exposed to endosulfan for 8 h at different doses (0.5 to 500 μM) relative to control (vehicle-treated) cells. The semi-log plots in the right column of Fig. 1 illustrate the corresponding percentages of metabolically viable cells as measured by quantification of NADH/NADPH levels relative to vehicle-treated control cells. These results show that hepatocytes are most resilient, whereas renal cells are most sensitive, to endosulfan insult. After exposure to endosulfan, hepatocytes showed no apparent LDH leakage at concentrations of up to 50 μM, but dramatic LDH leakage with cell death at higher concentrations. Renal cells showed no apparent LDH leakage after exposure to endosulfan at concentrations of 5 μM or less; however, LDH leakage and loss of cell viability became apparent after exposure at 10 μM. Cardiomyocytes showed no apparent LDH leakage at concentrations of up to 10 μM endosulfan, but showed LDH leakage and loss of cell viability after exposure at 20 μM.

We selected for each cell type a low and high dose to investigate gene expression changes induced by endosulfan exposure. The low dose was the highest concentration of endosulfan that might lead to little or no cell damage. The high dose was the minimum concentration of endosulfan that could result in apparent cell death. Table 1 shows the low and high doses selected for treatment of liver, heart, and kidney cells prior to RNA isolation.

3.2. DEGs induced by endosulfan exposure

We performed RNA-seq analysis to identify DEGs by comparing transcript abundance levels between cells exposed to and not exposed to endosulfan. We isolated RNA samples from primary cultures of rat hepatocytes, cardiomyocytes, and renal proximal tubular epithelial cells exposed to a low or high dose of endosulfan for 24 h (Table 1). Table 2 summarizes the numbers of DEGs, identified by using a false discovery rate (FDR) of 0.05 and a minimum gene expression fold change of 1.5 as the criteria for differential expression. In Table S1 of the Supplemental Materials, we provide details of each DEG, including its Entrez gene ID, gene name, gene symbol, p-value, FDR, and effect size (defined as the natural logarithm of fold change, ln(FC)).

Interestingly, we observed a strong correlation ($r = 0.98$) between the endosulfan dose and the number of DEGs, regardless of the organ of

Table 2
Number of differentially expressed genes (DEGs) associated with a 24-hour exposure of rat liver, heart, and kidney cells to endosulfan at the indicated concentrations.

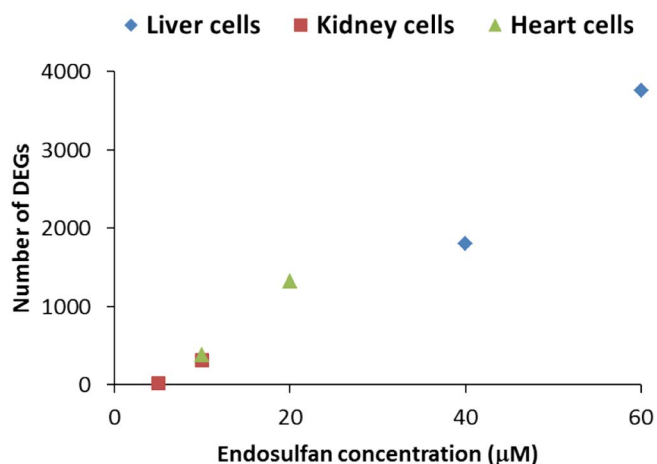| Cell type	Dose (μM)	DEGs
Cardiomyocytes	10	375
	20	1317
Hepatocytes	40	1807
	60	3763
Renal (proximal tubular epithelial cells)	5	22
	10	311

Fig. 2. Number of differentially expressed genes (DEGs) associated with exposure of rat liver, kidney, and heart cells to endosulfan at different concentrations. The figure shows a clear correlation between endosulfan concentration and the number of DEGs ($r = 0.98$).
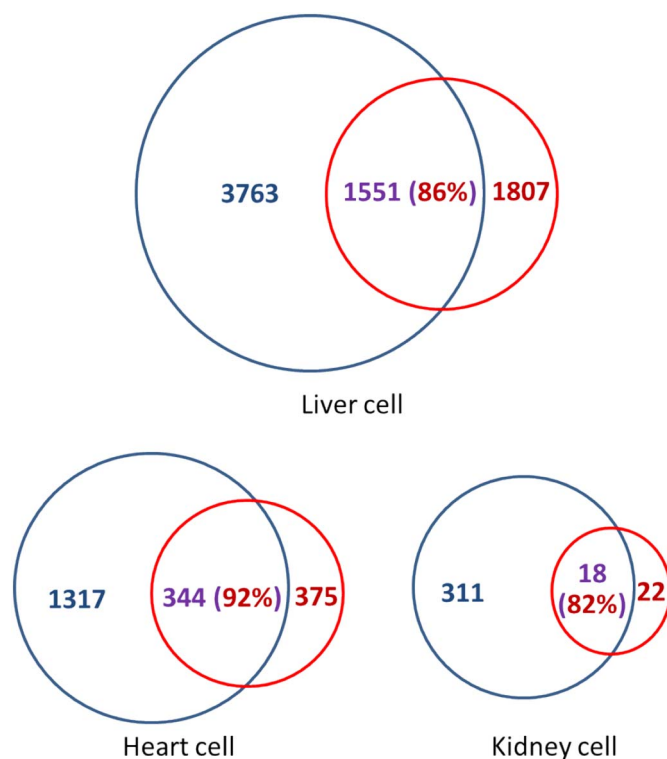

Fig. 3. Number of differentially expressed genes (DEGs) associated with high-dose (blue) and low-dose (red) treatments of rat liver, heart, and kidney cells. The numbers in purple are DEGs common to the high- and low-dose treatments (see Table S3 of the Supplemental Materials for lists of DEGs). The percentages in parentheses are of low-dose–associated DEGs, which were also expressed differentially in association with the corresponding high-dose treatments. (For interpretation of the references to color in this figure legend, the reader is referred to the web version of this article.)

origin of the cells (Fig. 2). Additionally, within each cell type, over 80% of the DEGs induced by the low dose also showed differential expression following the high-dose treatment (Fig. 3). However, the number of DEGs shared by all cell types was small, with only 5 at the low dose and 56 at the high dose (Fig. 4). These data suggest that cells of different organ origin respond to endosulfan insult differently.

Real-time qPCR analysis was performed to confirm several DEGs identified by the RNA-seq analysis using the same RNA samples that were isolated from primary cultures of rat hepatocytes, cardiomyocytes, and renal cells after 24 h of treatment with low or high dose endosulfan
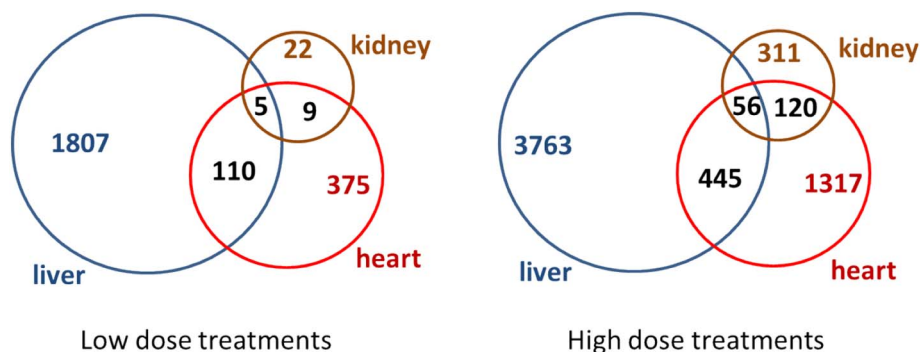
Fig. 4. Number of differentially expressed genes (DEGs) in rat liver, heart, and kidney cells exposed to endosulfan, common to low- and high-dose treatments. The relatively small number of common DEGs (see Table S4 of the Supplemental Materials for lists of DEGs) suggests that different cell types respond to endosulfan exposure differently.
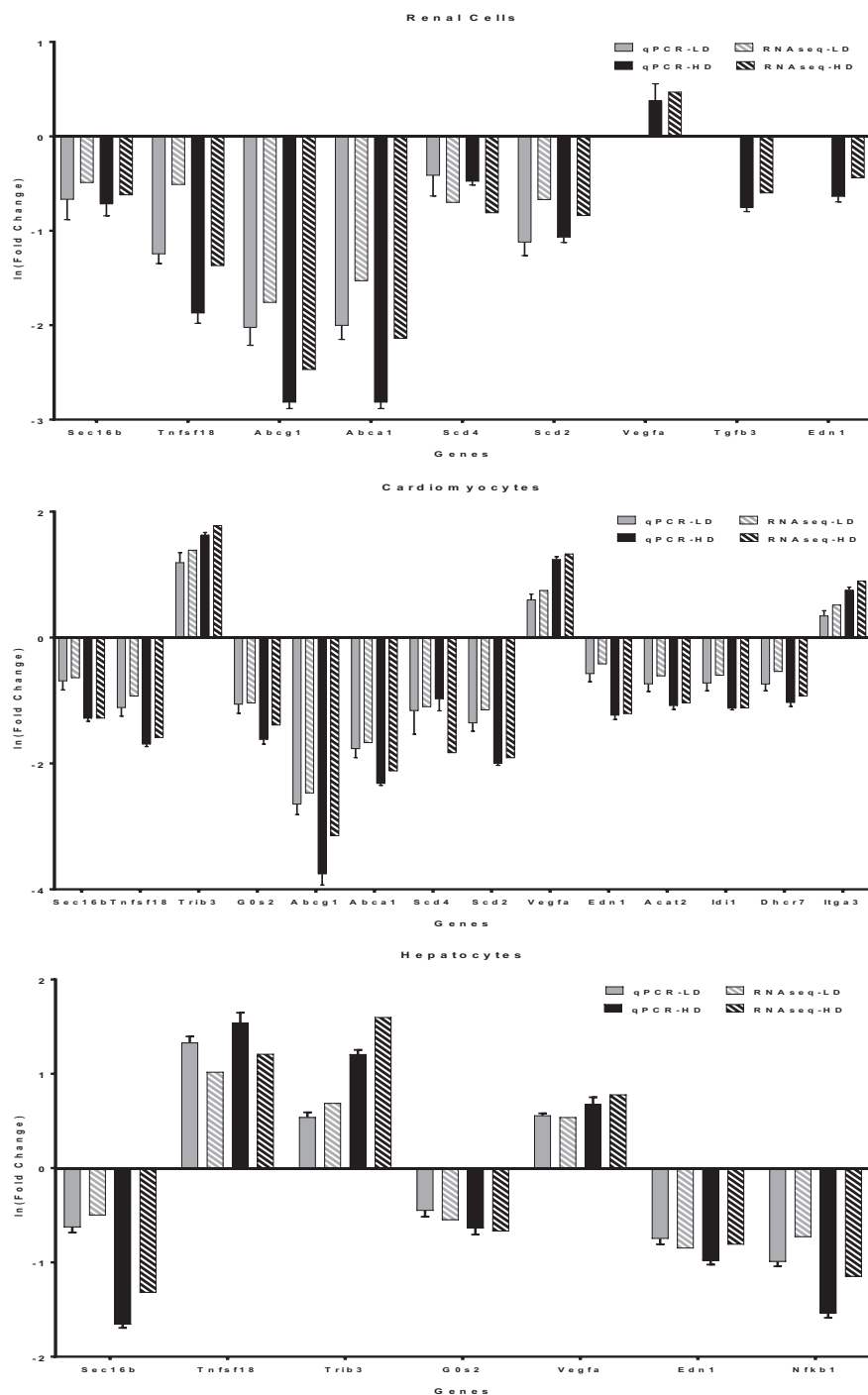

Fig. 5. A comparison between qPCR and RNA-seq differential gene expression data. Renal cells, cardiomyocytes and hepatocytes were treated 24 h with low dose (LD) or high dose (HD) endosulfan at the doses listed in Table 1. The natural logarithms of the average fold change (± SEM; n = 5 per group) in gene expression of endosulfan-treated relative to vehicle-treated cells were determined by real-time qPCR for several genes that were identified as DEGs after RNA-seq analysis. The qPCR values (solid shaded bars) are compared to the corresponding values determined by RNA-seq analysis (stripped shaded bars) for each treatment group within each cell type.

(see Table 1 for doses). A comparison between qPCR and RNA-seq differential gene expression data, reported as the natural logarithm of fold change, is illustrated in Fig. 5. The direction and magnitude of the fold change in gene expression of endosulfan-treated relative to vehicle-treated cells were comparable across the three cell types among the genes analyzed by qPCR and RNA-seq. The magnitude of the gene expression change was also dependent upon the treatment dose of endosulfan. Therefore, the qPCR data substantiates the RNA-seq analysis and the identification of DEGs associated with endosulfan treatment.

3.3. KEGG pathway enrichment analyses

Unlike most previous studies, which have investigated expression changes induced by endosulfan exposure for a small number of pre-selected genes or proteins, our RNA-seq experiments monitored the expression changes for thousands of genes, from which we identified a large number of DEGs. Instead of conducting detailed analyses of the responses of individual genes, which are prone to false discoveries due to noise in the data derived from high-throughput experiments, we performed KEGG pathway enrichment analysis on endosulfan-induced DEGs.

3.3.1. Genome-wide gene expression responses of kidney cells to endosulfan exposure

After a 24-h exposure of renal proximal tubular epithelial cells to 5 μM of endosulfan, only 22 genes showed significant alterations in expression levels (FDR < 0.05 and fold change ≥ 1.5). Of these 22 DEGs, the genes with the 2nd and 3rd largest fold changes in expression, but most reduced (5–6-fold), were Abcg1 and Abca1, respectively. These are genes for the functionally important ATP-binding cassette transporters involved in cellular cholesterol efflux. Thus, exposure to this low dose of endosulfan may affect kidney function with an accumulation of intracellular cholesterol, as has been seen with renal proximal tubular injury (Zager et al., 2003). The DEGs Scd2 and Scd4 also showed reduced expression with endosulfan treatment and encode stearoyl-CoA desaturase enzymes. These enzymes are key for cell survival by converting saturated fatty acids to monounsaturated fatty acids with their primary products, palmitoleic and oleic acids, providing major components of membrane phospholipids, triglycerides and cholesterol esters (Miyazaki et al., 2003). Besides the identification of these individual genes of interest, because the expression levels of only a small number of genes were significantly altered (22 DEGs), our pathway analyses did not identify any pathways significantly enriched with the DEGs.

Of the 311 DEGs identified in kidney cells exposed to 10 μM of endosulfan for 24 h, the ATP-binding cassette transporter genes, Abcg1 and Abca1, were again among those with the largest fold changes (reduced by approximately 12- and 8.5-fold, respectively). Likewise, as seen with the lower dose of endosulfan, the DEGs, Scd2 and Scd4, showed more than a 2-fold reduction in expression. Our KEGG pathway analysis indicated that DEGs were significantly enriched within three KEGG pathways – the rheumatoid arthritis, hypoxia-inducible factor 1 (HIF-1) signaling, and cytokine-cytokine receptor interaction pathways – with Benjamini false discovery rates (FDRs) of < 0.05, using DAVID bioinformatics online tools. The number of DEGs mapped to each of these pathways, their gene symbols, and Benjamini FDRs are given in Table 3.

3.3.2. Genome-wide gene expression responses of heart cells to endosulfan exposure

Exposing rat cardiomyocytes to a low dose of endosulfan (10 μM) for 24 h resulted in 375 DEGs, many of which were metabolic genes. The results of our KEGG pathway enrichment analyses are summarized in Table 4, which shows that the following pathways were significantly impacted by low-dose endosulfan exposure: the P450-mediated xenobiotic pathway, fatty-acid metabolism, and terpenoid backbone,

Table 3
KEGG pathways enriched by differentially expressed genes associated with 10-μM endosulfan treatment of rat kidney cells.

KEGG pathway	Mapped gene count	Benjamini FDR	Gene symbol	ln(FC)
Rheumatoid arthritis	9	0.004	Csf2	0.71
			Mmp3	0.61
			Vegfa	0.47
			Il1a	0.47
			Cd80	−0.42
			Angpt1	−0.49
			Il11	−0.52
			Cxcl12	−0.55
			Tgfb3	−0.60
HIF-1 signaling	8	0.043	Angpt4	1.05
			Eno2	0.52
			Vegfa	0.47
			Hk2	0.42
			Eif4ebp1	0.41
			Edn1	−0.44
			Angpt1	−0.49
			Pik3r3	−0.53
Cytokine-cytokine receptor interaction	10	0.049	Epor	0.81
			Csf2	0.71
			Il2rb	0.58
			Vegfa	0.47
			Il1a	0.47
			Il11	−0.52
			Cxcl12	−0.55
			Tgfb3	−0.60
			Ackr3	−0.72
			Tnfsf18	−1.37

antibiotic, and steroid biosynthesis pathways. These results indicate that although low-dose endosulfan exposure did not cause cell death, it significantly perturbed metabolic pathways.

Exposing rat cardiomyocytes to a high dose of endosulfan (20 μM) for 24 h resulted in 1317 DEGs. Some cell death was observed with high-dose endosulfan exposure. Table 4 shows the results of the pathway enrichment analyses. High-dose endosulfan exposure significantly impacted four KEGG pathways: the extracellular matrix (ECM)-receptor interaction, peroxisome proliferator-activated receptor (PPAR) signaling, antibiotic biosynthesis, and steroid biosynthesis pathways.

3.3.3. Genome-wide gene expression responses of liver cells to endosulfan exposure

The 40-μM (low) and 60-μM (high) doses of endosulfan applied to rat hepatocytes were the highest concentrations used in this study. These doses resulted in the highest number of DEGs. Applying the same criteria (FDR ≤ 0.05 and fold change ≥ 1.5), low-dose and high-dose exposures identified 1807 and 3763 DEGs, respectively. Table 5 shows the results of the pathway enrichment analyses. Given the number of DEGs identified with the treatment of liver cells, details of individual DEGs associated with each pathway are not listed in Table 5, but are given in Table S5 in the Supplemental Materials.

Low-dose exposure significantly enriched 15 KEGG pathways (Table 5), 10 of which were metabolic (biosynthesis and metabolism) pathways. Other pathways significantly enriched were those of ECM-receptor interaction, complement and coagulation cascades, and cytokine-cytokine receptor interaction. In contrast, high-dose exposure significantly enriched only 5 KEGG pathways: those of steroid hormone biosynthesis, ECM-receptor interaction, complement and coagulation cascades, cytokine-cytokine receptor interaction, and rheumatoid arthritis. The ECM-receptor interaction pathway was enriched in liver cells exposed to both 40 and 60 μM of endosulfan, as it was in cardiomyocytes exposed to 20 μM of endosulfan. Therefore, dysregulation of this pathway may contribute to endosulfan toxicity in liver cells as well as heart cells.

Table 4
KEGG pathways enriched by differentially expressed genes associated with 10- and 20-μM endosulfan treatment of rat heart cells.

KEGG pathway	Mapped gene count	Benjamini FDR	Gene symbol	ln(FC)
10-μM treatment				
Drug metabolism - cytochrome P450	7	0.024	Gsto2	2.26
			Gsta2	1.81
			Gsta5	1.10
			Gsta4	0.69
			Gstp1	0.66
			Fmo3	−0.54
			Fmo2	−0.58
Terpenoid backbone biosynthesis	6	0.028	Hmgcr	−0.48
			Fdps	−0.51
			Mvd	−0.59
			Idi1	−0.60
			Acat2	−0.61
			Hmgcs1	−0.69
Fatty-acid metabolism	9	0.032	LOC102549542	−0.51
			Acaca	−0.56
			Acat2	−0.61
			Acsl3	−0.63
			Fasn	−0.76
			Scd4	−1.10
			Scd2	−1.15
			Scd	−1.17
			LOC681458	−2.14
Biosynthesis of antibiotics	16	0.035	Uap1l1	0.72
			Aadat	0.62
			Cth	0.54
			Amdhd2	0.43
			Gfpt2	0.42
			Msmo1	−0.46
			Cyp51	−0.47
			Hmgcr	−0.48
			Hsd17b7	−0.50
			Acss2	−0.51
			Fdps	−0.51
			Mvd	−0.59
			Idi1	−0.60
			Acat2	−0.61
			Hmgcs1	−0.69
			Tm7sf2	−0.74
Steroid biosynthesis	5	0.039	Msmo1	−0.46
			Cyp51	−0.47
			Hsd17b7	−0.50
			Dhcr7	−0.54
			Tm7sf2	−0.74
20-μM treatment				

Table 4 (*continued*)

KEGG pathway	Mapped gene count	Benjamini FDR	Gene symbol	ln(FC)
Biosynthesis of antibiotics	38	2.4E−04	LOC100911625	2.26
			Aadat	1.60
			Uap1l1	1.18
			Gfpt2	1.04
			Cth	0.88
			Amdhd2	0.72
			Pla2g7	0.66
			Hk2	0.58
			Shmt1	0.55
			Ampd3	0.54
			Shmt2	0.54
			Phgdh	0.51
			Cat	0.47
			Galm	0.43
			Cmbl	0.41
			Pgm3	−0.44
			Ehhadh	−0.47
			Papss2	−0.49
			Mvk	−0.50
			Gfpt1	−0.55
			Pycr1	−0.56
			Acly	−0.58
			Sc5d	−0.63
			Idh1	−0.65
			Fdft1	−0.68
			Sqle	−0.69
			Msmo1	−0.82
			Aldoc	−0.82
			Cyp51	−0.84
			Acss2	−0.89
			Hsd17b7	−0.90
			Hmgcr	−0.91
			Mvd	−0.93
			Fdps	−0.98
			Acat2	−1.04
			Idi1	−1.12
			Tm7sf2	−1.20
			Hmgcs1	−1.24
ECM-receptor interaction	20	4.9E−04	Spp1	1.14
			Itgb7	1.10
			Itga3	0.90
			Cd36	0.60
			Itga7	0.58
			Cd44	0.57
			Dag1	0.55
			Lama3	0.54
			Reln	0.51
			Col27a1	−0.49
			Col6a2	−0.52
			Col3a1	−0.55
			Col5a1	−0.57
			Col5a3	−0.60
			Col6a1	−0.60
			Itga11	−0.64
			Tnn	−0.71
			Col6a6	−0.79
			Lamb3	−1.10
			Col4a3	−1.11
Steroid biosynthesis	9	1.6E−03	Tm7sf2	1.20
			Dhcr7	0.93
			Hsd17b7	0.90
			Cyp51	0.84
			Msmo1	0.82
			Sqle	0.69
			Fdft1	0.68
			Sc5d	0.63
			Ebp	0.52

Table 4 (*continued*)

KEGG pathway	Mapped gene count	Benjamini FDR	Gene symbol	ln(FC)
PPAR signaling	14	3.7E − 02	Fabp3	1.43
			Cyp4a3	0.86
			Cyp27a1	0.78
			Cd36	0.60
			Cpt1b	0.44
			Ehhadh	− 0.47
			Dbi	− 0.49
			Lpl	− 0.52
			Fads2	− 0.55
			Acsl3	− 0.99
			LOC681458	− 1.23
			Scd4	− 1.83
			Scd	− 1.87
			Scd2	− 1.91

Table 5
KEGG pathways enriched by differentially expressed genes associated with 40- and 60-µM endosulfan treatment of rat liver cells.

KEGG pathway	Mapped gene count	Benjamini-FDR
40-µM endosulfan treatment		
Steroid hormone biosynthesis	23	1.3E − 04
Chemical carcinogenesis	24	1.3E − 04
Retinol metabolism	21	2.0E − 04
ECM-receptor interaction	19	1.3E − 03
Amoebiasis	24	1.6E − 03
Metabolic pathways	184	1.1E − 02
Biosynthesis of antibiotics	46	1.3E − 02
Drug metabolism - cytochrome P450	16	1.4E − 02
Steroid biosynthesis	9	1.5E − 02
Cytokine-cytokine receptor interaction	29	1.8E − 02
Linoleic acid metabolism	11	1.8E − 02
Biosynthesis of amino acids	21	1.9E − 02
Complement and coagulation cascades	19	2.0E − 02
Arachidonic acid metabolism	15	2.7E − 02
Glutathione metabolism	15	3.4E − 02
60-µM endosulfan treatment		
ECM-receptor interaction	28	4.2E − 04
Cytokine-cytokine receptor interaction	47	1.6E − 02
Rheumatoid arthritis	26	2.1E − 02
Steroid hormone biosynthesis	27	3.7E − 02
Complement and coagulation cascades	28	3.7E − 02

4. Discussion

Although exposure to the pesticide endosulfan is known to be detrimental to human health and many toxicological studies have contributed to our knowledge of endosulfan action, insights into its molecular effects at sublethal doses remain poorly understood. The primary site of acute endosulfan toxicity is thought to be in the central nervous system, where endosulfan acts as a non-competitive gamma-aminobutyric acid (GABA) receptor antagonist, preventing the influx of chloride ions needed to inhibit neuronal firing; thus, endosulfan exposure leads to uncontrolled neuron excitation (Silva and Beauvais, 2010). With gradual accumulation of endosulfan within the body, renal, cardiac and hepatic toxicities have been reported (Menezes et al., 2017). To further investigate the underlying molecular mechanisms associated with endosulfan toxicity in these non-neuronal tissues, we applied the RNA-seq technique to investigate genome-wide gene expression changes in rat heart, liver, and kidney cells after 24 h of exposure to a low or high dose of endosulfan.

We found that kidney cells were most sensitive, and liver cells most resilient, to endosulfan exposure. A strong correlation was observed between the endosulfan dose and the number of DEGs. Within each cell type, over 80% of the DEGs induced by the low dose also showed differential expression following the high-dose treatment. Real-time qPCR

analysis confirmed several DEGs identified by RNA-seq with the direction and magnitude of the fold change in gene expression being comparable across liver, heart and kidney cells. KEGG pathway enrichment analysis of DEGs associated with endosulfan exposure showed that endosulfan treatment of both heart and liver cells mostly impacted metabolic pathways (Fig. 6). In contrast, very few pathways were enriched after endosulfan treatment of kidney cells. This difference may be attributed in part to the different endosulfan doses needed to induce injury in different cell types, as lower endosulfan doses led to smaller numbers of DEGs.

In rat cardiomyocytes our KEGG pathway enrichment analysis indicated that low-dose endosulfan exposure perturbed several metabolic pathways; the drug metabolism-cytochrome P450 pathway, fatty-acid metabolism, and terpenoid backbone, antibiotic, and steroid biosynthesis pathways. All the DEGs associated with the pathways for fatty-acid metabolism as well as terpenoid backbone and steroid biosynthesis had lower expression levels with endosulfan exposure. Within the drug metabolism pathway, the expression was decreased for flavin containing monooxygenase genes (Fmo2 and Fmo3) but increased for several glutathione S-transferase genes (Gsta5, Gsta2, Gsta4, Gstp1 and Gsto2). Glutathione S-transferase (GST) utilizes glutathione to detoxify substances that may arise from drug exposure or oxidative stress. Our increased expression of glutathione S-transferase genes agrees with previous reports of greater GST activity (Dong et al., 2013) and reduced glutathione levels (Hincal et al., 1995) with endosulfan exposure.

Within the biosynthesis of antibiotics pathway, most DEGs were expressed at lower levels with endosulfan exposure, but a few DEGs had greater levels of expression. These included the genes for glutamine:-fructose-6-phosphate amidotransferase 2 (Gfpt2) and uridine diphosphate-*N*-acetylglucosamine pyrophosphorylase 1 like 1 (Uap1l1) as well as cystathionine gamma-lyase (Cth). Cystathionine gamma-lyase by converting cystathionine to cysteine catalyzes the last step in the conversion of methionine to cysteine, which is a limiting substrate for the production of glutathione. Additionally, cystathionine gamma-lyase is the crucial enzyme for cardiovascular production of hydrogen sulfide, which exerts cardioprotective effects by activating the Nrf2/ARE pathway to promote antioxidant and anti-apoptotic molecule expression as well as inhibiting inflammatory signaling through the nuclear factor kappa B pathway (Huang et al., 2015).

Uridine diphosphate-*N*-acetylglucosamine pyrophosphorylase catalyzes the last step, whereas glutamine:fructose-6-phosphate amidotransferase (GFAT) catalyzes the first and rate-controlling step, of the hexosamine biosynthesis pathway, which converts fructose-6-phosphate to uridine diphosphate-*N*-acetylglucosamine, a precursor for the beta-O-linkage of *N*-acetylglucosamine (O-GlcNAc) modification of proteins. The O-GlcNAc post-translational modification may function as a stress signal, since O-GlcNAcylation increases in a dose-dependent manner in response to cellular stressors, such as oxidative stress, and augmenting O-GlcNAc levels promotes cell survival, whereas depressing O-GlcNAc levels reduces survival (Zachara and Hart, 2004). Endosulfan dose-dependently increased the expression of Gfpt2 and Uap1l1 in our studies of cardiomyocytes, which based on recent literature (Dassanayaka and Jones, 2014), would predict an increase of O-GlcNAc levels along with O-GlcNAcylation in order to provide protection from acute stress (hypoxia, ischemia, oxidative).

High-dose exposure of cardiomyocytes uniquely affected the ECM-receptor interaction and PPAR signaling pathways. PPARs are a group of nuclear receptor proteins that function as transcription factors, regulating the expression of genes that play essential roles in the regulation of cellular differentiation, development, and metabolism (Dunning et al., 2014; Michalik et al., 2006). Interactions between cells and the ECM are mediated by a number of transmembrane proteins that directly or indirectly control cellular activities, such as adhesion, migration, differentiation, proliferation, and apoptosis (Bonnans et al., 2014). Given their important roles, dysregulation of the ECM-receptor interaction and PPAR signaling pathways may be responsible for the

KEGG PATHWAY	HEART (10 µM)	HEART (20 µM)	KIDNEY (5 µM)	KIDNEY (10 µM)	LIVER (40 µM)	LIVER (60 µM)
XENOBIOTIC METABOLISM						
Glutathione metabolism					1	
Drug metabolism - cytochrome P450	1				1	
METABOLIC PATHWAYS						
Metabolic pathways					0	
Steroid biosynthesis	−1	−1			1	
Terpenoid backbone biosynthesis	−1					
Fatty acid metabolism	−1					
Biosynthesis of antibiotics	−1	−1			1	
Biosynthesis of amino acids					0	
LIVER METABOLISM						
Retinol metabolism					1	
Linoleic acid metabolism					1	
Steroid hormone biosynthesis					1	−1
Arachidonic acid metabolism					1	
CELLULAR RESPONSES						
ECM-receptor interaction		−1			−1	−1
Complement and coagulation cascades					−1	0
PPAR signaling pathway		−1				
Cytokine-cytokine receptor interaction				0	−1	−1
Rheumatoid arthritis				0		−1
SIGNAL TRANSDUCTION						
HIF-1 signaling				1		

Fig. 6. KEGG pathways affected by endosulfan exposure of rat liver, heart, and kidney cells. The Benjamini false discovery rates of all pathways shown are equal to or smaller than 0.05. The color and numerical value assigned to a cell type depends on the ratio of up-regulated to down-regulated genes mapped onto the pathways. If the number of up-regulated genes is significantly higher than that of down-regulated genes, the cell is colored pale green and assigned a value of 1. If the up-regulated genes are significantly fewer than the down-regulated genes, the cell is colored pink and assigned a value of −1. If the numbers of up- and down-regulated genes are about the same, the cell is colored yellow and assigned a value of 0. (For interpretation of the references to color in this figure legend, the reader is referred to the web version of this article.)

observed death of cardiomyocytes exposed to high-dose endosulfan.

How endosulfan may affect liver cells has been addressed previously using a genome-wide approach. Combining DNA microarray and mass spectrometry to identify cellular pathways altered by endosulfan exposure of a hepatocellular carcinoma cell line, HepG2, Gandhi et al. identified differentially expressed genes involved in metabolism, the immune/inflammatory response, and regulation of transcription and apoptosis (Gandhi et al., 2015). In a human-derived hepatocyte cell line, HepaRG, exposed to endosulfan in combination with 2,3,7,8 tet-rachlorodibenzo-p-dioxin, microarray analysis revealed changes in the expression of genes associated with hepatic intermediary metabolic pathways (Ambolet-Camoit et al., 2015). Using a metabonomic approach to identify plasma, bone marrow and liver biomarkers associated with low dose exposure to endosulfan, Canlet et al. identified metabolite changes associated with oxidative stress in the liver as well as altered glucose and lipid metabolism (Canlet et al., 2013). A genome-wide approach was also taken in *Drosophila melanogaster* exposed to endosulfan, using microarray based gene expression profiling, differentially expressed genes involved in development, metabolism, immune response and oxidative stress were identified (Sharma et al., 2011). These reports suggest that endosulfan exposure commonly alters pathways associated with oxidative stress and inflammatory signaling and has profound effects on metabolic pathways.

Our genome-wide RNA-seq approach support these observations with identification of several common metabolic pathways that were impacted by endosulfan exposure in liver as well as heart cells. In addition, we found that the ECM-receptor interaction pathway was also enriched by endosulfan exposure in both liver and heart cells. Previous studies have shown that at the concentrations we used for the heart and liver cells (20–60 µM), endosulfan is cytotoxic to many cell types. For instance, 20 µM of endosulfan reportedly caused cytotoxic effects in rat testicular cells (Sinha et al., 1999; Sinha et al., 2001). At 40 to 60 µM, endosulfan inhibited the growth of human umbilical vein endothelial cells (Li et al., 2015), and an IC$_{50}$ of 49 µM was reported for the cytotoxicity of endosulfan on HepG2 cells (Sohn et al., 2004). Given that endosulfan is cytotoxic to various cells at these concentrations, a common molecular mechanism may underlie the shared cytotoxicity. Disruption of ECM-receptor interaction may serve as such a mechanism, because the ECM plays an important role in maintaining cell structure and function, and most animal cells can only grow in vitro when they are attached to surfaces through the ECM (Kim et al., 2011). In fact, endosulfan was reported to increase anoikis, cell death by inappropriate or loss of cell adhesion, in HepG2 cells (Peyre et al., 2012). We observed in liver and heart cells reduced expression of collagen genes and altered expression of integrin genes with endosulfan exposure that could lead to disruption of the ECM, loss of cell adhesion and increased anoikis. Enrichment of these high-dose (20 to 60 µM) endosulfan-associated DEGs of heart and liver cells to the ECM-receptor interaction pathway

suggests that disruption of the ECM may be a common molecular mechanism of endosulfan cytotoxicity.

In contrast to the relatively high doses of endosulfan used in heart and liver cells, kidney cells were exposed to the lowest endosulfan concentrations (5 and 10 μM) and showed the smallest number of DEGs. Two identified DEGs, Abca1 and Abcg1, encode adenosine triphosphate binding cassette transporter A1 and G1, respectively, that are involved in cellular cholesterol efflux. After a 24-h exposure of renal proximal tubular epithelial cells to endosulfan at the lowest dose used in our study, Abca1 and Abcg1 gene expression was reduced by 5–6-fold. This would predict that endosulfan would lead to a reduction in cholesterol efflux transport, and thereby accumulation of intracellular cholesterol. Within 18–24 h following renal proximal tubular injury, free and esterified cholesterol accumulates as efflux of cholesterol is reduced (Zager et al., 2003). In cultured human proximal tubular epithelial cells exposed to hyperglycemia and in kidneys of mice with diabetes, especially diabetic mice with nephropathy, the expression of Abca1 and Abcg1 is reduced (Tsun et al., 2014). Interestingly, both in mice and human diabetic nephropathy, the expression of liver X receptor alpha (LXRα), whose activity promotes the expression of Abca1 and Abcg1, is also reduced (Herman-Edelstein et al., 2014; Tsun et al., 2014). The expression of two other genes, Scd4 and Scd2, were reduced with endosulfan treatment, and like Abca1 and Abcg1, LXRα activity promotes greater expression levels. Pregnane X receptor (PXR) may inhibit LXRα transcriptional activation (Jeske et al., 2017), thus increased PXR activity would reduce LXRα dependent gene expression. Endosulfan is a ligand of the PXR receptor and increases PXR activity (Casabar et al., 2010), which may result in lower LXRα activity and reduced expression of LXRα target genes like Abca1, Abcg1, SCD4 and SCD2.

At the low dose endosulfan concentration, with a small number of DEGs, we were unable to identify pathways affected by endosulfan. However, at the high dose (10 μM) of endosulfan, the concentration was sufficient to induce a greater number of DEGs that were significantly enriched to the rheumatoid arthritis, cytokine-cytokine receptor interaction, and hypoxia-inducible factor 1 (HIF-1) signaling pathways. The rheumatoid arthritis and cytokine-cytokine receptor interaction pathways are immune response pathways. It is not surprising that some immune response pathways are activated in endosulfan-treated cells, given that chronic and acute renal diseases, irrespective of the initiating cause, share inflammation and immune system activation as common underlying mechanisms (Imig and Ryan, 2013). The HIF-1 signaling pathway was uniquely activated in kidney cells. HIF-1 is a transcription factor whose target genes encode proteins that increase oxygen delivery and mediate adaptive responses to oxygen deprivation, thereby influencing cell growth, differentiation, and apoptosis (Cavadas et al., 2015; Maxwell et al., 2001). The positive fold change in the expression of several HIF-1 target genes (vascular endothelial growth factor and angiopoietin) after exposure to endosulfan suggests that HIF-1 signaling is activated. Previous studies have found that oxidative stress is a key molecular initiating event of endosulfan toxicity (Kannan et al., 2000; Kannan and Jain, 2003; Sohn et al., 2004). As pointed out by Blokhina and coworkers, excessive generation of reactive oxygen species, i.e., oxidative stress, is an integral part of hypoxia (Blokhina et al., 2003). Hypoxia activates HIF-1 signaling to protect cells from excessive oxidative stress and support cell survival functions, such as, increasing the cellular capacity for anaerobic glycolysis to generate ATP. In this context, our data derived from the kidney cells are in agreement with previous findings that oxidative stress is a key molecular initiating event of endosulfan toxicity.

5. Summary

Endosulfan has been the subject of many toxicology studies. However, the molecular mechanisms underlying the toxicity of endosulfan to animals and humans are still not fully understood. Here, we used primary cells from rat kidney, heart and liver to examine the effects of direct exposure of cells derived from these organs to known doses of endosulfan. In addition, we used state-of-the-art RNA-seq technology to investigate genome-wide gene expression changes associated with endosulfan exposure to identify molecular mechanisms that might warrant future in vivo investigation. We found that kidney cells were the most sensitive, and liver cells the most resilient, to endosulfan exposure. Exposure of kidney cells to low concentrations of endosulfan led to differentially expressed genes, some of which were significantly enriched in the HIF-1 signaling pathway. Endosulfan-induced changes in the expression level of genes within this pathway suggest that oxidative stress underlies toxicity in kidney cells. Similar analyses of differentially expressed genes also showed that exposure to higher concentrations of endosulfan could lead to dysregulation of the ECM-receptor interaction pathway in heart and liver cells. Thus, results of these studies suggest two distinct molecular mechanisms underlying endosulfan cytotoxicity: oxidative stress as indicated by endosulfan-induced activation of the HIF-1 signaling pathway in the case of kidney cells, and disruption of the ECM in the case of heart and liver cells. Because the kidney cells were most sensitive to endosulfan, the kidney is likely a primary target organ of endosulfan exposure. However, future animal studies are needed to confirm these findings and test the proposed models of endosulfan cytotoxicity derived from our primary cell studies. Although, the cytotoxic effects of endosulfan we observed in heart and liver cells may not be observed in vivo, because kidney injury would likely develop before endosulfan concentrations could reach a level sufficient to induce heart or liver damage.

Supplementary data to this article can be found online at https://doi.org/10.1016/j.tiv.2018.01.022.

Conflict of interest

The authors declare that there are no conflicts of interest.

Transparency document

The Transparency document associated with this article can be found in online version.

References

Ambolet-Camoit, A., Ottolenghi, C., Leblanc, A., Kim, M.J., Letourneur, F., Jacques, S., Cagnard, N., Guguen-Guillouzo, C., Barouki, R., Aggerbeck, M., 2015. Two persistent organic pollutants which act through different xenosensors (alpha-endosulfan and 2,3,7,8 tetrachlorodibenzo-p-dioxin) interact in a mixture and downregulate multiple

genes involved in human hepatocyte lipid and glucose metabolism. Biochimie 116, 79–91. http://dx.doi.org/10.1016/j.biochi.2015.07.003.

Blokhina, O., Virolainen, E., Fagerstedt, K.V., 2003. Antioxidants, oxidative damage and oxygen deprivation stress: a review. Ann. Bot. 91 Spec No, 179–194.

Bonnans, C., Chou, J., Werb, Z., 2014. Remodelling the extracellular matrix in development and disease. Nat. Rev. Mol. Cell Biol. 15, 786–801. http://dx.doi.org/10.1038/nrm3904.

Bray, N.L., Pimentel, H., Melsted, P., Pachter, L., 2016. Near-optimal probabilistic RNA-seq quantification. Nat. Biotechnol. 34, 525–527. http://dx.doi.org/10.1038/nbt.3519.

Canlet, C., Tremblay-Franco, M., Gautier, R., Molina, J., Metais, B., Blas, Y.E.F., Gamet-Payrastre, L., 2013. Specific metabolic fingerprint of a dietary exposure to a very low dose of endosulfan. J. Toxicol. 2013 (545802). http://dx.doi.org/10.1155/2013/545802.

Casabar, R.C., Das, P.C., Dekrey, G.K., Gardiner, C.S., Cao, Y., Rose, R.L., Wallace, A.D., 2010. Endosulfan induces CYP2B6 and CYP3A4 by activating the pregnane X receptor. Toxicol. Appl. Pharmacol. 245, 335–343. http://dx.doi.org/10.1016/j.taap.2010.03.017.

Cavadas, M.A., Mesnieres, M., Crifo, B., Manresa, M.C., Selfridge, A.C., Scholz, C.C., Cummins, E.P., Cheong, A., Taylor, C.T., 2015. REST mediates resolution of HIF-dependent gene expression in prolonged hypoxia. Sci. Rep. 5 (17851). http://dx.doi.org/10.1038/srep17851.

Dassanayaka, S., Jones, S.P., 2014. O-GlcNAc and the cardiovascular system. Pharmacol. Ther. 142, 62–71. http://dx.doi.org/10.1016/j.pharmthera.2013.11.005.

Demeter, J., Heyndrickx, A., 1978. Two lethal endosulfan poisonings in man. J. Anal. Toxicol. 2, 68–74.

Dong, M., Zhu, L., Shao, B., Zhu, S., Wang, J., Xie, H., Wang, J., Wang, F., 2013. The effects of endosulfan on cytochrome P450 enzymes and glutathione S-transferases in zebrafish (Danio rerio) livers. Ecotoxicol. Environ. Saf. 92, 1–9. http://dx.doi.org/10.1016/j.ecoenv.2012.10.019.

Dunning, K.R., Anastasi, M.R., Zhang, V.J., Russell, D.L., Robker, R.L., 2014. Regulation of fatty acid oxidation in mouse cumulus-oocyte complexes during maturation and modulation by PPAR agonists. PLoS One 9, e87327. http://dx.doi.org/10.1371/journal.pone.0087327.

Ely, T.S., Macfarlane, J.W., Galen, W.P., Hine, C.H., 1967. Convulsions in thiodan workers. A preliminary report. J. Occup. Med. 9, 35–37.

Gandhi, D., Tarale, P., Naoghare, P.K., Bafana, A., Krishnamurthi, K., Arrigo, P., Saravanadevi, S., 2015. An integrated genomic and proteomic approach to identify signatures of endosulfan exposure in hepatocellular carcinoma cells. Pestic. Biochem. Physiol. 125, 8–16. http://dx.doi.org/10.1016/j.pestbp.2015.06.008.

Guo, F.Z., Zhang, L.S., Wei, J.L., Ren, L.H., Zhang, J., Jing, L., Yang, M., Wang, J., Sun, Z.W., Zhou, X.Q., 2016. Endosulfan inhibiting the meiosis process via depressing expressions of regulatory factors and causing cell cycle arrest in spermatogenic cells. Environ. Sci. Pollut. Res. Int. 23, 20506–20516. http://dx.doi.org/10.1007/s11356-016-7195-y.

Herman-Edelstein, M., Scherzer, P., Tobar, A., Levi, M., Gafter, U., 2014. Altered renal lipid metabolism and renal lipid accumulation in human diabetic nephropathy. J. Lipid Res. 55, 561–572. http://dx.doi.org/10.1194/jlr.P040501.

Hincal, F., Gurbay, A., Giray, B., 1995. Induction of lipid peroxidation and alteration of glutathione redox status by endosulfan. Biol. Trace Elem. Res. 47, 321–326. http://dx.doi.org/10.1007/BF02790133.

Huang da, W., Sherman, B.T., Lempicki, R.A., 2009. Systematic and integrative analysis of large gene lists using DAVID bioinformatics resources. Nat. Protoc. 4, 44–57. http://dx.doi.org/10.1038/nprot.2008.211.

Huang, S., Li, H., Ge, J., 2015. A cardioprotective insight of the cystathionine gamma-lyase/hydrogen sulfide pathway. Int. J. Cardiol. Heart Vasc. 7, 51–57. http://dx.doi.org/10.1016/j.ijcha.2015.01.010.

Imig, J.D., Ryan, M.J., 2013. Immune and inflammatory role in renal disease. Compr. Physiol. 3, 957–976. http://dx.doi.org/10.1002/cphy.c120028.

Jeske, J., Bitter, A., Thasler, W.E., Weiss, T.S., Schwab, M., Burk, O., 2017. Ligand-dependent and -independent regulation of human hepatic sphingomyelin phosphodiesterase acid-like 3A expression by pregnane X receptor and crosstalk with liver X receptor. Biochem. Pharmacol. 136, 122–135. http://dx.doi.org/10.1016/j.bcp.2017.04.013.

Jonsson, C.M., Toledo, M.C., 1993. Bioaccumulation and elimination of endosulfan in the fish yellow tetra (*Hyphessobrycon bifasciatus*). Bull. Environ. Contam. Toxicol. 50, 572–577.

Kannan, K., Jain, S.K., 2003. Oxygen radical generation and endosulfan toxicity in Jurkat T-cells. Mol. Cell. Biochem. 247, 1–7.

Kannan, K., Holcombe, R.F., Jain, S.K., Alvarez-Hernandez, X., Chervenak, R., Wolf, R.E., Glass, J., 2000. Evidence for the induction of apoptosis by endosulfan in a human T-cell leukemic line. Mol. Cell. Biochem. 205, 53–66.

Kim, S.H., Turnbull, J., Guimond, S., 2011. Extracellular matrix and cell signalling: the dynamic cooperation of integrin, proteoglycan and growth factor receptor. J. Endocrinol. 209, 139–151. http://dx.doi.org/10.1530/JOE-10-0377.

Kim, H.G., Kim, Y.R., Park, J.H., Khanal, T., Choi, J.H., Do, M.T., Jin, S.W., Han, E.H., Chung, Y.H., Jeong, H.G., 2015. Endosulfan induces COX-2 expression via NADPH oxidase and the ROS, MAPK, and Akt pathways. Arch. Toxicol. 89, 2039–2050. http://dx.doi.org/10.1007/s00204-014-1359-7.

Li, S., Xu, D., Guo, J., Sun, Y., 2015. Inhibition of cell growth and induction of

inflammation by endosulfan in HUVEC-C cells. Environ. Toxicol. http://dx.doi.org/10.1002/tox.22180.

Lutter, C., Iyengar, V., Barnes, R., Chuvakova, T., Kazbekova, G., Sharmanov, T., 1998. Breast milk contamination in Kazakhstan: implications for infant feeding. Chemosphere 37, 1761–1772.

Maier-Bode, H., 1968. Properties, effect, residues and analytics of the insecticide endosulfan. Residue Rev. 22, 1–44.

Maxwell, P.H., Pugh, C.W., Ratcliffe, P.J., 2001. Activation of the HIF pathway in cancer. Curr. Opin. Genet. Dev. 11, 293–299.

McIntyre, L.M., Lopiano, K.K., Morse, A.M., Amin, V., Oberg, A.L., Young, L.J., Nuzhdin, S.V., 2011. RNA-seq: technical variability and sampling. BMC Genomics 12 (293). http://dx.doi.org/10.1186/1471-2164-12-293.

Menezes, R.G., Qadir, T.F., Moin, A., Fatima, H., Hussain, S.A., Madadin, M., Pasha, S.B., Al Rubaish, F.A., Senthilkumaran, S., 2017. Endosulfan poisoning: an overview. J. Forensic Legal Med. 51, 27–33. http://dx.doi.org/10.1016/j.jflm.2017.07.008.

Mersie, W., Seybold, C.A., McNamee, C., Lawson, M.A., 2003. Abating endosulfan from runoff using vegetative filter strips: the importance of plant species and flow rate. Agric. Ecosyst. Environ. 97, 215–223. http://dx.doi.org/10.1016/S0167-8809(03)00035-5.

Michalik, L., Auwerx, J., Berger, J.P., Chatterjee, V.K., Glass, C.K., Gonzalez, F.J., Grimaldi, P.A., Kadowaki, T., Lazar, M.A., O'Rahilly, S., Palmer, C.N., Plutzky, J., Reddy, J.K., Spiegelman, B.M., Staels, B., Wahli, W., 2006. International Union of Pharmacology. LXI. Peroxisome proliferator-activated receptors. Pharmacol. Rev. 58, 726–741. http://dx.doi.org/10.1124/pr.58.4.5.

Miyazaki, M., Jacobson, M.J., Man, W.C., Cohen, P., Asilmaz, E., Friedman, J.M., Ntambi, J.M., 2003. Identification and characterization of murine SCD4, a novel heart-specific stearoyl-CoA desaturase isoform regulated by leptin and dietary factors. J. Biol. Chem. 278, 33904–33911. http://dx.doi.org/10.1074/jbc.M304724200.

Oberg, A.L., Bot, B.M., Grill, D.E., Poland, G.A., Therneau, T.M., 2012. Technical and biological variance structure in mRNA-Seq data: life in the real world. BMC Genomics 13, 304. http://dx.doi.org/10.1186/1471-2164-13-304.

Peyre, L., Zucchini-Pascal, N., de Sousa, G., Rahmani, R., 2012. Effects of endosulfan on hepatoma cell adhesion: epithelial-mesenchymal transition and anoikis resistance. Toxicology 300, 19–30. http://dx.doi.org/10.1016/j.tox.2012.05.008.

Pimentel, H.J., Bray, N., Puente, S., Melsted, P., Pachter, L., 2016. Differential Analysis of RNA-Seq Incorporating Quantification Uncertainty. bioRxivorg. http://dx.doi.org/10.1101/058164.

Reuber, M.D., 1981. The role of toxicity in the carcinogenicity of endosulfan. Sci. Total Environ. 20, 23–47.

Sharma, A., Mishra, M., Ram, K.R., Kumar, R., Abdin, M.Z., Chowdhuri, D.K., 2011. Transcriptome analysis provides insights for understanding the adverse effects of endosulfan in *Drosophila melanogaster*. Chemosphere 82, 370–376. http://dx.doi.org/10.1016/j.chemosphere.2010.10.002.

Silva, M.H., Beauvais, S.L., 2010. Human health risk assessment of endosulfan. I: toxicology and hazard identification. Regul. Toxicol. Pharmacol. 56, 4–17. http://dx.doi.org/10.1016/j.yrtph.2009.08.013.

Sinha, N., Adhikari, N., Narayan, R., Saxena, D.K., 1999. Cytotoxic effect of endosulfan on rat Sertoli-germ cell coculture. Reprod. Toxicol. 13, 291–294.

Sinha, N., Adhikari, N., Saxena, D.K., 2001. Effect of endosulfan on the enzymes of polyol pathway in rat sertoli-germ cell coculture. Bull. Environ. Contam. Toxicol. 67, 821–827.

Sohn, H.Y., Kwon, C.S., Kwon, G.S., Lee, J.B., Kim, E., 2004. Induction of oxidative stress by endosulfan and protective effect of lipid-soluble antioxidants against endosulfan-induced oxidative damage. Toxicol. Lett. 151, 357–365. http://dx.doi.org/10.1016/j.toxlet.2004.03.004.

Song, M.O., Lee, C.H., Yang, H.O., Freedman, J.H., 2012. Endosulfan upregulates AP-1 binding and ARE-mediated transcription via ERK1/2 and p38 activation in HepG2 cells. Toxicology 292, 23–32. http://dx.doi.org/10.1016/j.tox.2011.11.013.

Tsun, J.G., Yung, S., Chau, M.K., Shiu, S.W., Chan, T.M., Tan, K.C., 2014. Cellular cholesterol transport proteins in diabetic nephropathy. PLoS One 9, e105787. http://dx.doi.org/10.1371/journal.pone.0105787.

Wei, J., Zhang, L., Ren, L., Zhang, J., Yu, Y., Wang, J., Duan, J., Peng, C., Sun, Z., Zhou, X., 2017. Endosulfan inhibits proliferation through the Notch signaling pathway in human umbilical vein endothelial cells. Environ. Pollut. 221, 26–36. http://dx.doi.org/10.1016/j.envpol.2016.08.083.

Zachara, N.E., Hart, G.W., 2004. O-GlcNAc a sensor of cellular state: the role of nucleocytoplasmic glycosylation in modulating cellular function in response to nutrition and stress. Biochim. Biophys. Acta 1673, 13–28. http://dx.doi.org/10.1016/j.bbagen.2004.03.016.

Zager, R.A., Johnson, A.C., Hanson, S.Y., Shah, V.O., 2003. Acute tubular injury causes dysregulation of cellular cholesterol transport proteins. Am. J. Pathol. 163, 313–320. http://dx.doi.org/10.1016/S0002-9440(10)63655-3.

Zhang, L., Wei, J., Ren, L., Zhang, J., Wang, J., Jing, L., Yang, M., Yu, Y., Sun, Z., Zhou, X., 2017a. Endosulfan induces autophagy and endothelial dysfunction via the AMPK/mTOR signaling pathway triggered by oxidative stress. Environ. Pollut. 220, 843–852. http://dx.doi.org/10.1016/j.envpol.2016.10.067.

Zhang, L., Wei, J., Ren, L., Zhang, J., Yang, M., Jing, L., Wang, J., Sun, Z., Zhou, X., 2017b. Endosulfan inducing apoptosis and necroptosis through activation RIPK signaling pathway in human umbilical vascular endothelial cells. Environ. Sci. Pollut. Res. Int. 24, 215–225. http://dx.doi.org/10.1007/s11356-016-7652-7.